

## 3D Simulation of Charge Transfer in a Gas Electron Multiplier (GEM) and Comparison to Experiment<sup>1</sup>

Archana SHARMA<sup>2</sup>

CERN, Geneva Switzerland & GSI Darmstadt, Germany

### *Abstract*

*A 3-dimensional simulation of the electric field and avalanche propagation in a Gas Electron Multiplier (GEM) is performed. Results on charge transport are compared to experiment and agree within experimental errors; avalanche mechanism and positive ion feedback are studied. The possibilities of single photon detection with full efficiency from internal photocathodes are investigated.*

---

<sup>1</sup> Paper presented at the Symposium on Applications of Particle Detectors in Medicine, Biology and Astrophysics, Siegen, Germany, 6-8 October 1999.

<sup>2</sup> Address for Correspondence CERN, CH 1211, Geneva, Switzerland  
e-mail Archana.Sharma@cern.ch

## 1. Introduction

In the last few years a variety of micropattern detectors [1] has invaded the scene of charged particle tracking in a hostile high luminosity environment replacing the traditional multiwire chambers with their higher rate. Made with simple printed circuit board technology, with through holes etched on double sided metallized Kapton foils typically 50  $\mu\text{m}$  thick, the Gas Electron Multiplier (GEM) [2] has been demonstrated to be a robust charged particle detector. Two foils in cascade form a Double GEM [3-5], delimited by a drift electrode above the first foil and a signal collection electrode below the second. Due to its design, positive ion feedback into the drift is reduced as compared to that of a wire chamber [6]. In this work a first attempt is made to model the operation of a GEM using a 3D simulation. The electron drift properties are investigated and transparency has been computed and compared to experimental results; gain and positive ion feedback are also estimated.

## 2. GEM Operation: 2D model and its shortcomings

Fig.1 shows the 2D electric field in a single GEM computed using MAXWELL [7] and GARFIELD [8]. The geometry used throughout this work is as follows unless stated otherwise: 70  $\mu\text{m}$  metal hole diameter, 140  $\mu\text{m}$  pitch with staggered rows. With appropriate potentials on the drift electrodes and across the GEM, and a grounded collection electrode, electrons enter the drift volume and are multiplied in the high electric fields in the GEM channels ( $E_H$ ). The resulting avalanche of electrons provides sufficient gain for charged particle detection.

## 3. Three dimensional model of GEM and Electric Fields

A 3D model was made using MAXWELL field simulator. The model consists of a basic mirror symmetric cell and volume, with a drift and collection electrode on the top and bottom respectively [9]. The field computed by using the 3D model differs from that of the 2D as exemplified in Fig. 2. This is due to the metallic surfaces present both on top and the bottom of the GEM unaccounted for in the 2D model, as well as the double conical Kapton well on either side. The electric fields computed by Maxwell are imported in Garfield for subsequent electron transport study. Fig. 3 shows drift of electrons created by a track; one can appreciate the 3D nature of the problem, observing that some of them go into neighboring staggered holes.

### 3.1 Transparency of the GEM

More than on individual fields, the electrical transparency of the GEM depends on the ratio of drift to the dipole field ( $E_D/E_H$ ), and its optical transparency [10]; a staggered matrix increases transparency as compared to straight rows of holes. Relative measurements of electrical transparency have been reported [10]. Within the 3D model, transparency has been computed generating uniformly a matrix of 2500 electrons on the drift electrode surface and following their path as they drift and diffuse down the channel<sup>3</sup>. Fig. 4 shows the computed versus measured transparency for a single GEM. The experimental values fall between those computed for holes with 70  $\mu\text{m}$  and 80  $\mu\text{m}$  diameter. This could well be the tolerance of the manufacturing process. Calculations for transparency in a non-zero magnetic field will be presented in section 4.

---

<sup>3</sup> The Monte Carlo version of electron drift was used in Garfield.

### 3.2 Avalanche, Effective Gain and Positive Ions

The previous sections described how electrons move from the drift region into the GEM channels, and accounted for the loss of the electrons simply due to drift and diffusion. When electrons encounter the high field in the holes, they experience ionizing collisions thereby resulting in an avalanche of electrons, whose size depends on the dipole field. Some of the electrons of the avalanche are lost to the bottom electrode of the GEM, consequently the ‘effective’ or visible gain of the multiplier is lower than the total number of ionizing collisions effected by a single electron [5]. The reliability of computations in this respect is quite low, since the Townsend coefficient is not very well known at high fields [11]; gains obtained from calculations differ up to factors of 2-3 when increasing the GEM voltage, as shown in Fig.5. Detailed understanding of this discrepancy is being studied. The majority of the electrons are produced in the center; a doughnut of electron production is seen at the lower metal edge, where the electric field is higher. This is a totally local effect; diffusion completely overtakes the field structure in GEM and  $\sim 200 \mu\text{m}$  below the GEM surface there is no trace of this effect; thus obliterating the GEM structure for any localization measurements. This results in making the mechanical alignment between two foils (Double GEM) redundant. Positive ions are produced essentially in the whole channel but mostly in the vicinity of the lower GEM electrode; and move to the drift volume, the fraction depending strongly on the drift field [10]. It should be noted however, that the signal detected on readout (strips/pads) is totally due to electron collection, there is no slow component due to the positive ion movement as compared to a traditional MWPC sense wire signal <sup>4</sup>. The time taken by the positive ions to reach the GEM top typically corresponds to a few  $\mu\text{s}$  and few tens of  $\mu\text{s}$  to reach the drift electrode. The fractional number of positive ion feedback was also verified for a couple of voltage settings points at low drift fields, in general the agreement with [10] is within 20%, as shown in Fig. 6.

### 4. Operation of GEM in a high Magnetic Field

The qualitative behavior of performance in the presence of a strong electric field perpendicular to the drift field was investigated with the 2D model [10]; see fig. 7. Despite several drift lines ending on the bottom of the foil, the lateral spread of the avalanche is enough to compensate for the loss of electrons due to the Lorentz force. Fig. 8 shows the computed transparency and gain as a function of magnetic field (perpendicular to the electric field) with an Ar-CO<sub>2</sub> (70-30) gas mixture, and the electric field values as shown in the inset. One can see that while transparency drops dramatically, (note that for these computations, a low drift field was chosen); there is no perceivable effect on the gain; measurements reporting no efficiency drop in the presence of a magnetic field have been published earlier [4]. The gas mixture as well as field configuration is by no means optimized; more work is needed in this direction.

### 5. Single electron/photon detection with a Gas Electron Multiplier

Large gains have been reported earlier in pure noble gases with single and cascaded GEMs [12]. Single photoelectrons from an internal photocathode may be detected exploiting the large diffusion in pure argon and having electric fields setup such that the amplification is divided into two parts: parallel plate mode in the drift and subsequent avalanche development in the channel. Efficiency was investigated, especially for the worst point of the photocathode, namely that equidistant from the centers of three adjacent holes. 200 avalanches were generated from electrons distributed along a line on the photocathode corresponding to that drawn from the centre of a hole to the worst point described above.

---

<sup>4</sup> The signal will also depend on the pre-amplifier shaping time, an effect which is not discussed here.

When diffusion is switched off in the program, one gets the expected low values for transparency, see curve 2 in Fig. 9. With an overall gain of the order of few tens, in the total system (drift + GEM), there is however a non zero number of electrons transmitted through the channel; curve 1. From lines 1 and 3, one can see that the number of collected electrons increases slightly off the centre of the GEM hole, due to the slightly higher fields and then this number drops since the field lines end up on the metal surface. Moving further along this line, the slight increase is due to the fact that more electrons find neighboring holes as another row of staggered holes is made available. When gain is high, these variations are obliterated by the avalanche statistics and diffusion: line 3 of the figure shows that the variation is much smaller. Nevertheless one needs to increase the overall electric field in the system, raising the probability of photon feedback. Therefore a compromise has to be found between gain variation and total efficiency for single electron transfer, obviously an experimental issue.

Fig. 10 shows the efficiency as a function of  $\langle N \rangle$ , ( $N$  being the number of electrons transmitted through the channel for each avalanche) computed only for electrons starting from this worst point on the photocathode. It is seen that for low visible gains, the efficiency is approximately 70-80 %, while once  $\langle N \rangle$  reaches around 50, the efficiency is 98%, and then does not vary with gain. Therefore, given a minimum effective gain, an almost fully efficient electron detection is predicted using a noble gas.

## References

- [1] F. Sauli and A. Sharma CERN-EP/99-69, Submitted to Ann. Rev. Nucl. And Part. Sci. May 1999.
- [2] F. Sauli, Nucl. Instr. And Meth. A386(1997)531
- [3] J. Benlloch et al, IEEE Trans. Nucl. Sci. NS-45 (1998)531
- [4] C. Büttner et al, Nucl. Instr. And Meth. A409(1998)79
- [5] J. Benlloch et al, Nucl. Instr. And Meth. A419(1998)410
- [6] F. Sauli, CERN-EP-TA1, Gem Readout of the Time Projection Chamber, Internal Report (1999)
- [7] MAXWELL Commercial Finite Element Computation Package, Ansoft Co. Pittsburg, PA
- [8] GARFIELD CERN Wire Chamber Field & Transport Computation Program written by R. Veenhof, Version 6.33
- [9] T. Motos-Lopez and A. Sharma CERN-IT/99-5
- [10] S. Bachmann et al CERN-EP/99-48, Submitted Nucl. Instr. And Meth. (1999)
- [11] F. Sauli and A. Sharma Nucl. Instr. And Meth. A 323(1992)280-283
- [12] A. Buzulutskov et al, The GEM photomultiplier operated with noble gas mixtures, Subm. Nucl. Instr. And Meth. (1999).

## Figure Captions

- Fig. 1 Principle of the GEM drift lines computed from a 2D Electric Field.
- Fig. 2 Comparison of 2D and 3D electric field computed along the GEM channel.
- Fig. 3 Drift of electrons from a track into several GEM holes, the holes have been sketched by hand to guide the eye.
- Fig. 4 Computed and measured transparency.
- Fig. 5 Effective Gain computation and measurements.
- Fig. 6 Positive ion feedback into the drift volume, induction field: field between GEM and anode structure.
- Fig. 7 Drift lines in a magnetic field perpendicular to drift direction.

- Fig. 8 Transparency and gain as a function of magnetic field (open circles for transparency, closed circles for gain).
- Fig. 9 Average number of electrons from an avalanche transferred through the GEM channel as a function of the distance from the centre of a hole and the point equidistant from three adjacent holes.
- Fig. 10 Efficiency as a function of the average number of electrons transmitted through the channel.

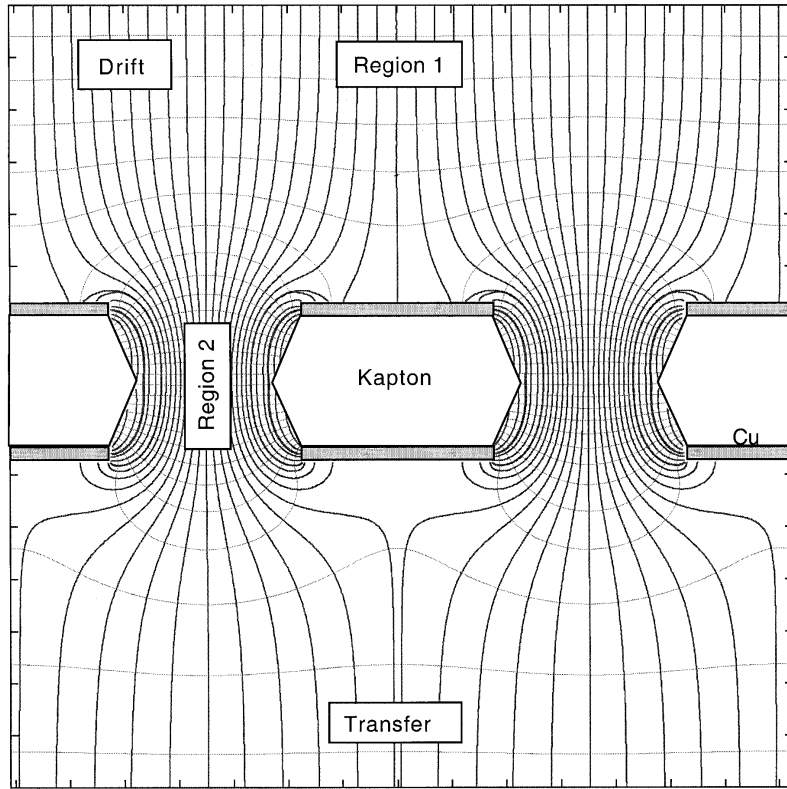


Fig. 1

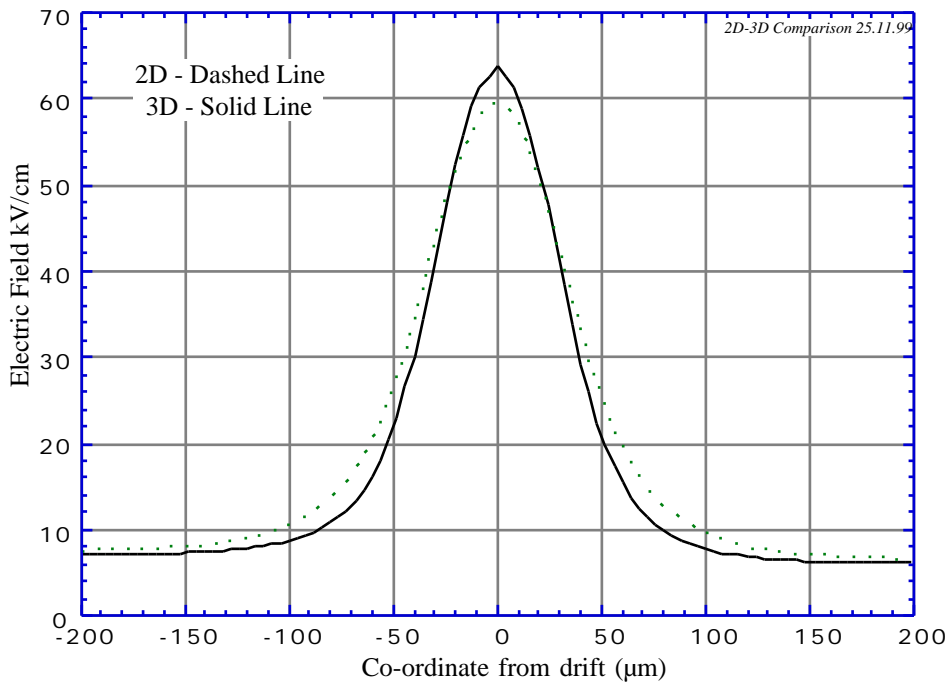


Fig. 2

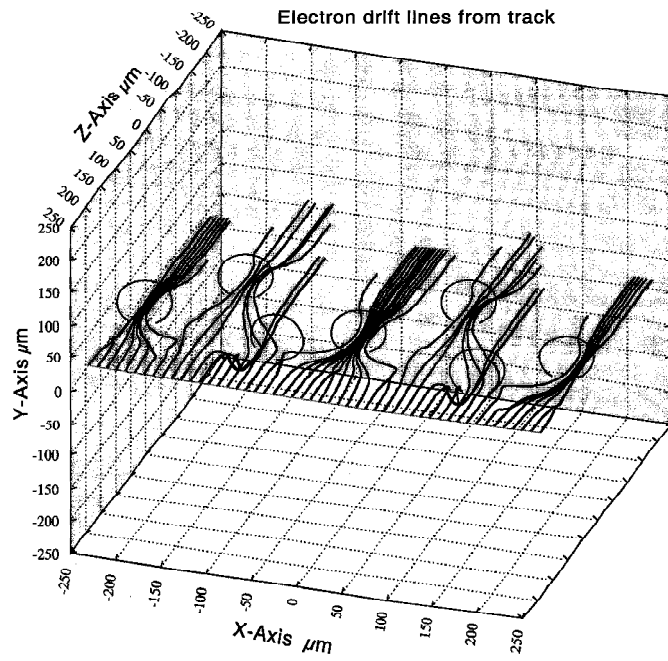


Fig. 3

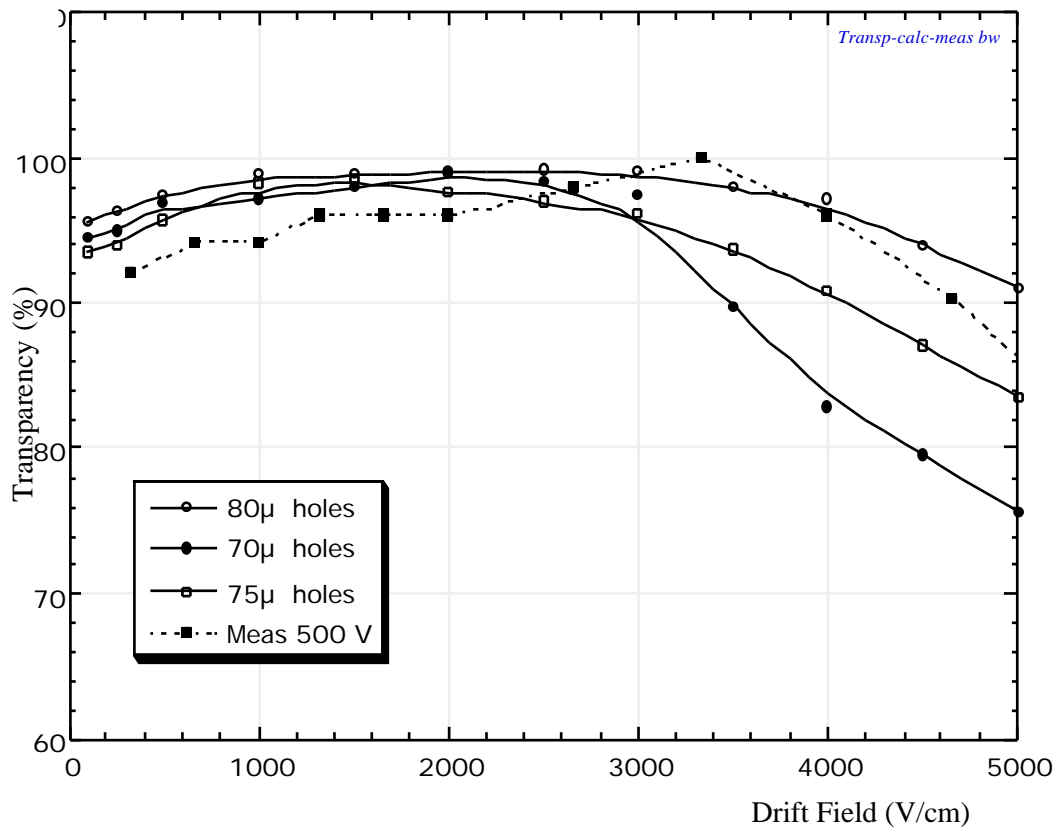


Fig. 4

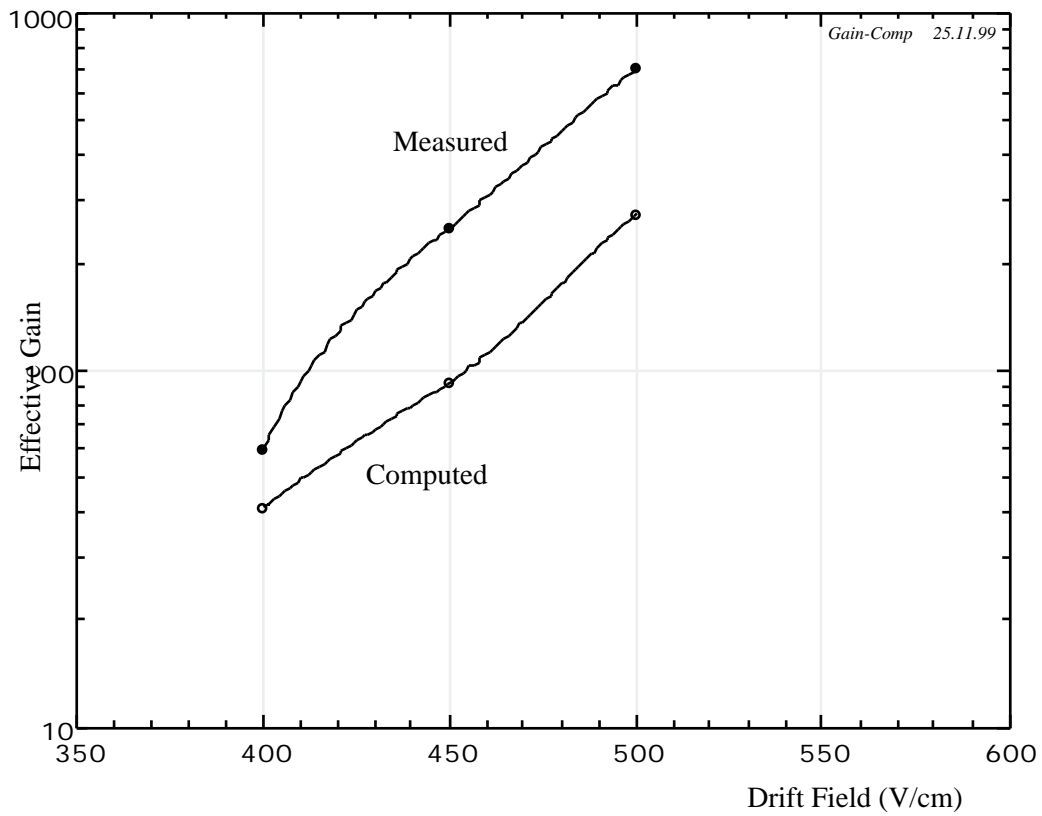


Fig. 5

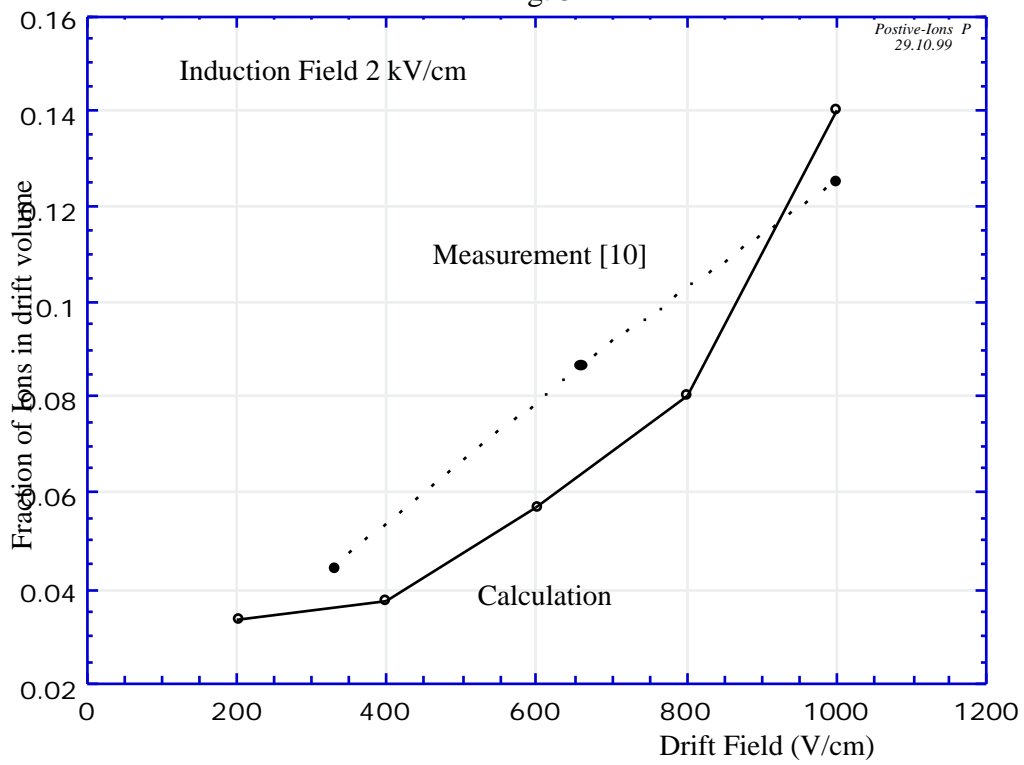


Fig. 6

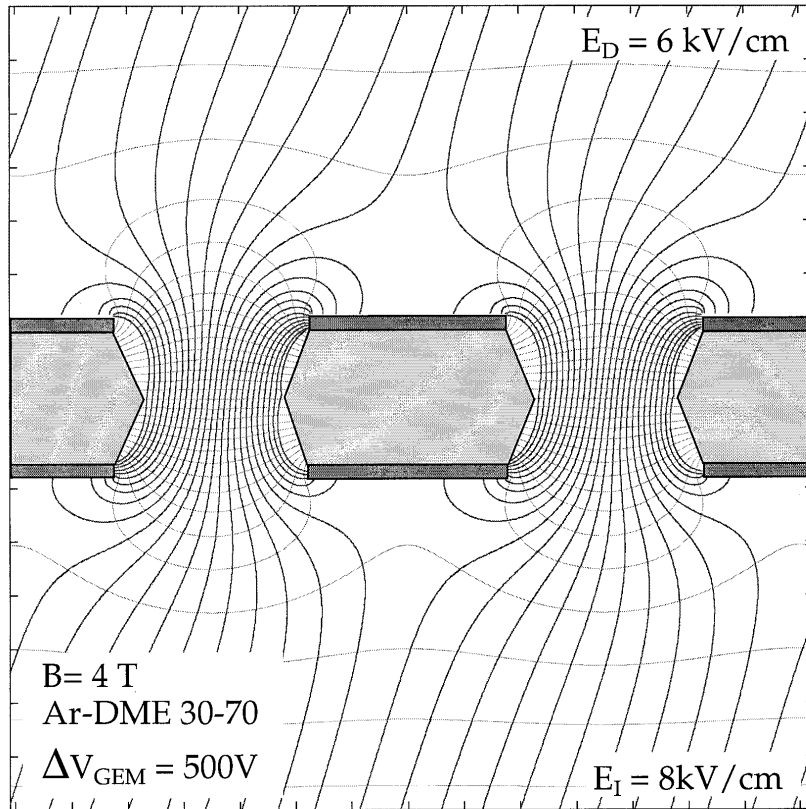


Fig. 7

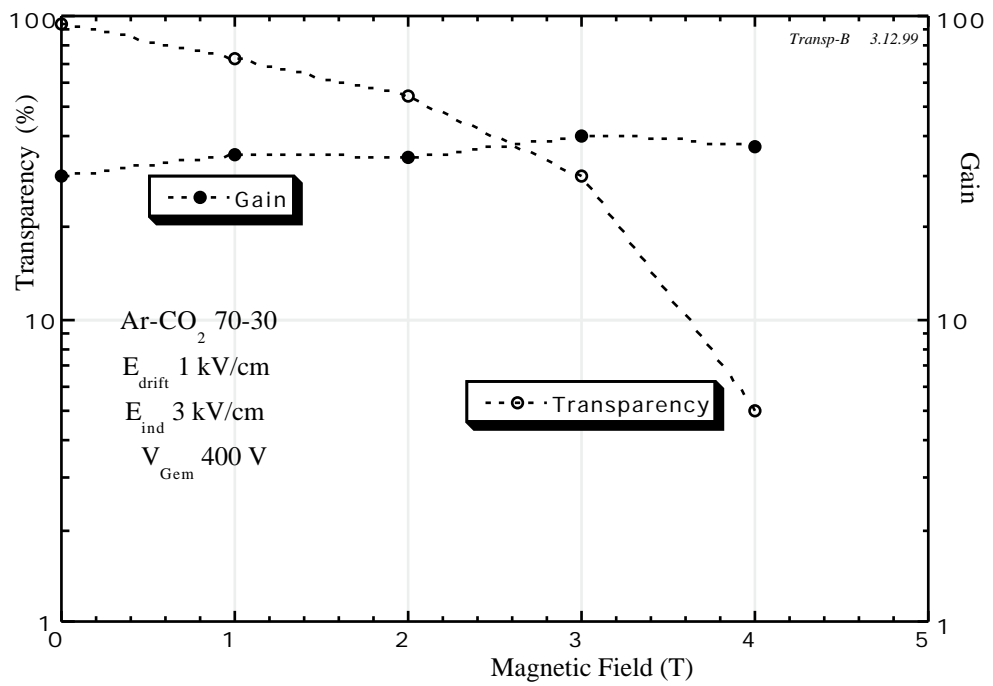


Fig. 8

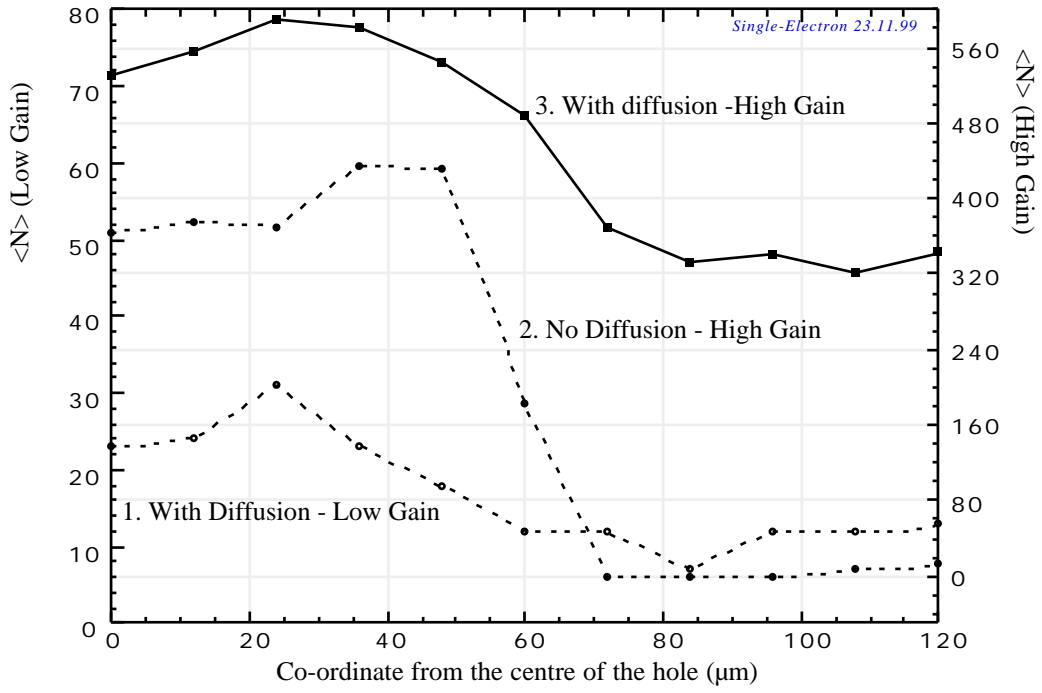


Fig. 9

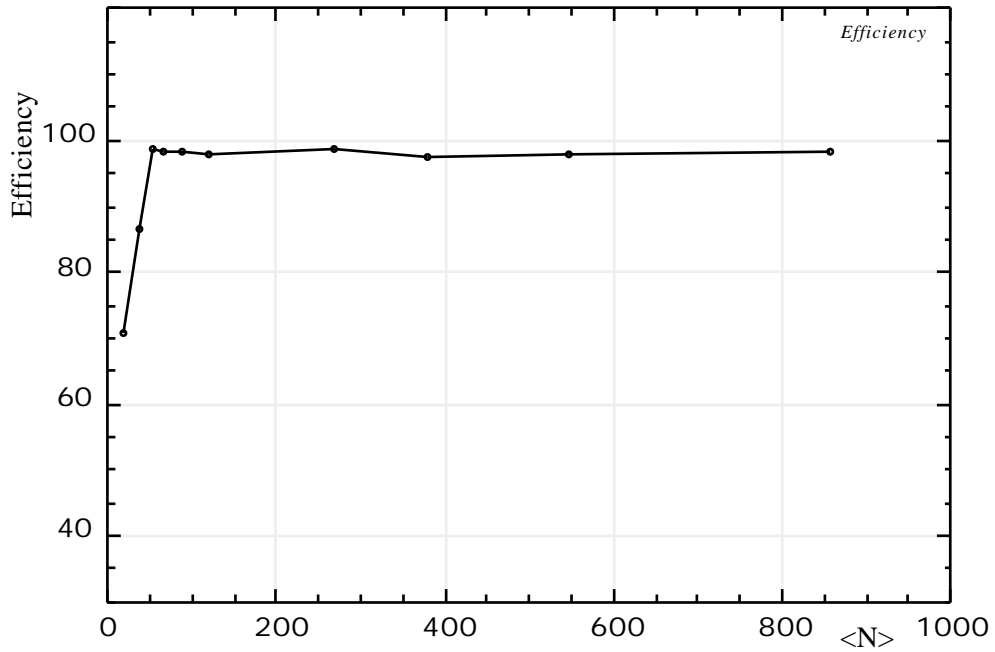


Fig. 10